Eur. Phys. J. B **24**, 443–456 (2001)

THE EUROPEAN PHYSICAL JOURNAL B

EDP Sciences

$(Sr/Ca)_{14}Cu_{24}O_{41}$ spin ladders studied by NMR under pressure

Y. Piskunov[1], D. Jérome[1,a], P. Auban-Senzier[1], P. Wzietek[1], C. Bourbonnais[2], U. Ammerhal[3,4], G. Dhalenne[3], and A. Revcolevschi[3]

[1] Laboratoire de Physique des Solides[b], Université Paris-Sud, 91405, Orsay, France
[2] Département de Physique, Université de Sherbrooke, Sherbrooke, Québec, J1K2R1, Canada
[3] Laboratoire de Chimie des Solides[c], Université Paris-Sud, 91405, Orsay, France
[4] II. Physikalisches Institut, Universität zu Köln, Zülpicher Str. 77, 50937 Köln, Germany

Received 8 March 2001 and Received in final form 27 July 2001

Abstract. ^{63}Cu-NMR measurements have been performed on two-leg hole-doped spin ladders $Sr_{14-x}Ca_xCu_{24}O_{41}$ single crystals $0 \leq x \leq 12$ at several pressures up to the pressure domain where the stabilization of a superconducting ground state can be achieved. The data reveal a marked decrease of the spin gap derived from Knight shift measurements upon Ca substitution and also under pressure and confirm the onset of low lying spin excitations around P_c as previously reported. The spin gap in $Sr_2Ca_{12}Cu_{24}O_{41}$ is strongly reduced above 20 kbar. However, the data of an experiment performed at $P = 36$ kbar where superconductivity has been detected at 6.7 K by an inductive technique have shown that a significant amount of spin excitations remains gapped at 80 K when superconductivity sets in. The standard relaxation model with two and three-magnon modes explains fairly well the activated relaxation data in the intermediate temperature regime corresponding to gapped spin excitations using the spin gap data derived from Knight shift experiments. The data of Gaussian relaxation rates of heavily doped samples support the limitation of the coherence length at low temperature by the average distance between doped holes. We discuss the interplay between superconductivity and the spin gap and suggest that these new results support the exciting prospect of superconductivity induced by the interladder tunneling of preformed pairs as long as the pressure remains lower than the pressure corresponding to the maximum of the superconducting critical temperature.

PACS. 74.25.Ha Magnetic properties – 74.72.Jt Other cuprates – 76.60.Cq Chemical and Knight shifts

1 Introduction

The discovery of a superconducting state under pressure in a hole-doped spin-ladder cuprate $Sr_{14-x}Ca_xCu_{24}O_{41}$ with $x = 13.6$ (sintered powder) [1] and $x = 11.5$ (single crystal) [2], has renewed the interest for superconductivity in low dimensional systems and its interplay with magnetism. These systems can be viewed as a link between high T_c cuprates and quasi one dimensional organics which are two classes of exotic superconductors where the mechanism of superconductivity is still highly debated [3,4].

Undoped spin-ladders of general formula $Sr_nCu_{n+1}O_{2n+1}$, where the copper valence is exactly 2 (Cu^{2+} with spin $S = 1/2$), consist of cuprate ladder planes separated by Sr layers [5,6]. Their magnetic properties depend on the number of legs in the ladders [3]. In case of an even number of legs the formation of spin singlets on each rung leads to the opening of a spin gap in the spin excitations. In the two-leg ladder compound $SrCu_2O_3$ the spin gap can be seen by the exponential drop of the spin susceptibility [7]. This singlet ground state is not possible for an odd number of legs and a finite value of the spin susceptibility is reached at low temperature for instance in the three-leg compound $Sr_2Cu_3O_5$ [7].

The $Sr_{14-x}Ca_xCu_{24}O_{41+\delta}$ series has a more complicated structure built from the piling up of CuO_2 chains, Sr (or Ca) and Cu_2O_3 two-leg ladders layers with an orthorhombic symmetry [8]. The interlayer distance (along the b axis), which is 1.6 Å in $x = 0$ compound, is shortened upon Ca substitution. Moreover, there is a misfit between the lattice parameters of chains and ladders sublattices ($10 \times c_{\text{chain}} = 7 \times c_{\text{ladder}}$). This system is inherently hole doped as the stoichiometry implies an average copper valence of 2.25. However, optical measurements [9] have shown that holes for the $x = 0$ compound are residing mainly in the chains leading in turn to an insulating behavior and to a magnetic ordering revealed by neutron scattering experiments [10] with a valence of 2.06 for the Cu ladder sites. Then, although Ca and Sr are

[a] e-mail: jerome@lps.u-psud.fr
[b] UMR 8502
[c] UMR 8648

isovalent atoms, holes are transfered from the chains to the ladders upon Ca substitution. Consequently, the copper valence in the ladders increases from 2.06 up to 2.20 (0.2 hole per Cu) as x increases from 0 to 11 [9]. At the same time, the longitudinal conductivity (along the c axis) increases, leading to quasi one dimensional ($Q-1-D$) metallic properties [11,12]. It has been suggested that holes doped into the ladders will share common rungs since it is the configuration which minimizes the number of damaged spin singlets, [13]. As far as the transverse a-axis is concerned, a confinement of holes pairs on the ladders takes place below a confinement temperature called $T^{\star}$ which is above room temperature for all samples with $x \leq 8$ and drops to below 300 K for $x = 12$. However, as for undoped ladder compounds, a spin gap is still observed in the ladder plane and a smaller spin gap ($\approx$ 140 K) is also present in the chain sublattice. The existence of a spin gap on ladders was demonstrated by ^{63}Cu-NMR measurements which can easily separate the contributions coming from copper nuclei belonging to chains and ladders. The spin part of the NMR shift, which is directly proportional to the spin susceptibility, allows an accurate determination of these gaps. Upon Ca substitution, the amplitude of the spin gap in the ladders decreases from 500 K [14,15] or 430 K [16] for $x = 0$ down to 250 K for $x = 12$ [15,16] while it remains practically unchanged in the chains (125−140 K) [14,16]. Therefore, the spin gapped structure survives the existence of a finite concentration of holes in the ladders in agreement with theoretical suggestions [13,17,18]. For samples with the largest Ca concentration, an applied pressure in the range 30−80 kbar stabilizes a superconducting ground state in the ladder planes with a transition temperature passing through a maximum at 10 K around 40 kbar [12].

The great interest of superconducting spin ladders lies in the theoretical prediction of superconductivity in the d-wave channel which is a direct consequence of the spin gapped character of the magnetic excitations [13]. The possible link between the predicted superconducting (SC) phase of isolated ladders and the SC phase stabilized under high pressure in $(Sr/Ca)_{14}Cu_{24}O_{41}$ is therefore a challenge in the physics of strongly correlated low dimensional fermions.

An early pressure study carried out on $Sr_2Ca_{12}Cu_{24}O_{41}$ [19] concluded to the existence of low lying spin excitations under high pressure conditions *i.e.* $P = 30-32$ kbar when superconductivity appears at $T_c \approx 5$ K. However, recent NMR studies at 17 kbar and inelastic neutron scattering experiments at 21 kbar argued that the spin gap does not change under pressure [20–22]. Consequently, it is a very important matter to study how the transient domain between the spin gap regime and the situation with low lying spin excitations develops under pressure.

The compound $La_5Ca_9Cu_{24}O_{41}$ also investigated in this work is the closest to the situation of the undoped spin ladders although displaying the chains and ladders structure similar to the $(Sr/Ca)_{14}Cu_{24}O_{41}$ series with an average Cu valence of 2.04 as compared to 2.25 in the latter series [23,10].

Our work presents the results of a study of the whole $Sr_{14-x}Ca_xCu_{24}O_{41}$ series (called Cax from now on) including the parent compound $La_5Ca_9Cu_{24}O_{41}$ [23] (La5) *via* NMR shifts and relaxation measurements under pressure up to 36 kbar which is a pressure well above the critical pressure ($\approx$ 30 kbar) needed for the stabilization of superconductivity in $Sr_2Ca_{12}Cu_{24}O_{41}$. Some preliminary measurements performed on Ca12 only up to 32 kbar have appeared in reference [24]. Section 2 provides some experimental details. NMR shifts and relaxation results are presented in Section 3. These results are discussed in Section 4, in terms of magnon excitations in undoped and doped spin ladders. We shall see how this picture breaks down when the superconducting phase is approached. The interpretation of the Gaussian relaxation time in Section 5 provides an access to the spin correlation length. Finally, the relation between spin gap and pressure-induced superconductivity is discussed in the Section 6.

2 Experimental

Experiments have been carried out on single crystalline samples of $Sr_{14-x}Ca_xCu_{24}O_{41}$ ($x = 0, 2, 5, 8, 9, 12$) and $La_5Ca_9Cu_{24}O_{41}$ grown by the traveling solvent floating zone method [10]. ^{63}Cu($I = 3/2$) NMR measurements have been performed at a fixed magnetic field of 9.3 tesla ($B \parallel b$) *via* a Fourier transform of the spin echo on the central transition $(1/2, -1/2)$ using phase alternation techniques. The echo signal was obtained after the pulse sequence $(\tau_p)_x - t_{\rm del} - (\tau_p)_y - t - echo$ with $\tau_p \leq 1.5$ μs. The Q-factor of the resonance circuit did not exceed 50. This provides a rather uniform irradiation of the central line for the measurements down to 80 K. The broad ^{63}Cu spectrum at low temperature was obtained by summing up the Fourier transforms of spin echo signals taken at different frequencies with a frequency increment such as $\Delta\nu_{\rm in} \sim 100 \div 150$ kHz which is kept smaller than the full-width at half-maximum (FWHM) of a single Fourier spectrum. The possible influence of the phase adjustment on the line shape for each Fourier transformed subspectra was minimized in the following way. The resonance circuit was tuned at every step $\Delta\nu_{\rm in}$. A subspectrum was obtained at a fixed phase and then was passed through a rectangular band-pass digital filter $(-1.7\Delta\nu_{\rm in}; +1.7\Delta\nu_{\rm in})$. The comparison between different spectra $\sim (U^2_{\chi'} + U^2_{\chi''})^{1/2}$ shows that the peak position can be measured with an accuracy of $\pm$25 kHz.

NMR data have been obtained in a seemingly non magnetic high hydrostatic pressure cell. However, in order to take into account the unavoidable slight shift of the external field generated by the tungsten carbide piston close to the sample, the NMR signal from the copper RF coil has been used as a field marker (known to be only weakly pressure dependent) [25]. The influence of the piston was manifested in an additional T-independent positive shift of the resonance frequency for ^{63}Cu in the RF

coil, $^{63}\nu$(metal), remaining within $\Delta\nu_{\rm add} \sim 120 \div 170$ kHz depending on pressure as well as in a slight broadening of the ^{63}Cu(metal) NMR line from 20 kHz (FWHF) (without piston) to 30 kHz in the presence of the piston. The FWHM of ^{63}Cu(metal) spectra never exceeded 50 kHz at any pressure and temperature. Consequently, we can be confident that all shifts or line broadenings reported in this study exceeding 50 kHz are related to intrinsic properties of the samples. Shift values reported in this work have been calculated relative to the ^{63}Cu resonance in a diamagnetic substance, namely $^{63}\nu_0 = ^{63}\nu$(metal)/1.0023, where $^{63}\nu$(metal) is the resonance frequency of copper metal nuclei. The magnetic shift of the ^{63}Cu-NMR line was determined using a simulation software taking into account quadrupolar corrections to the Zeeman frequency in a second order perturbation theory.

For a magnetic field B parallel to the α-axis of the sample the resonance frequency of the central transition reads [26,27],

$$\nu_{(1/2,-1/2),\alpha} = (1+K_\alpha)\nu_0 + \frac{(\nu_\beta - \nu_\gamma)^2}{12\nu_0\,(1+K_\alpha)} \qquad (1)$$

where K_α, ν_0, $\nu_{\beta,\gamma}$ are the NMR shift, the Larmor frequency in a diamagnetic substance and the quadrupolar tensor components respectively.

For a magnetic field B parallel to the b-axis of the sample (*i.e.* the transverse axis corresponding to the alternate packing axis of chains and ladders) the resonance frequency of the central transition reads,

$$\nu_{(1/2,-1/2),b} = (1+K_b)\nu_0 + \frac{(\nu_c - \nu_a)^2}{12\nu_0\,(1+K_b)}\,. \qquad (2)$$

Following the determination of the quadrupole tensor in $Sr_{2.5}Ca_{11.5}Cu_{24}O_{41}$ [15], the second term in equation (2) amounts to 42 kHz (400 ppm) with a negligible temperature dependence as compared to the temperature dependence of the first contribution since $(\nu_c - \nu_a)$ remains practically temperature independent [16].

The pressure dependence of the quadrupolar contribution is not easy to estimate. However, considering the 100 ppm change of the quadrupolar contribution at $B = 9.3$ T($\parallel b$) which is observed upon Ca substitution between $x = 0$ and $x = 11.5$ in $Sr_{14-x}Ca_xCu_{24}O_{41}$ [16,15] and the expected equivalence between the chemical pressure of Ca and the applied pressure which is a result of the present study we can conclude that a change of the quadrupolar term exceeding 100 ppm in 32 kbar is very unlikely .

The ^{63}Cu Knight shift is very anisotropic in spin ladders. Hence, a precise orientation of the single crystal in the magnetic field along the corresponding axis is requested for the determination of the actual $^{63}K_\alpha(T)$ temperature dependence. The situation $B = 9.3$ T($\parallel b$) which maximizes the value of the total shift has been reached through a fine adjustment of the angular position of the pressure cell in the magnetic field.

Under some circumstances, line shifts and broadenings at low temperature both exceed largely 50 kHz. Since the ^{63}Cu(metal) NMR line does not broaden significantly below 50 K under any pressure, the drastic broadening of lines taking place at low T cannot be explained by the external field generated by the piston. This broadening is thus an intrinsic property of ladders. Very similar features have been reported in the NMR study of Zn-doped $SrCu_2O_3$ [28].

Measurements of the spin-lattice relaxation time T_1 have been performed in the same field of $B = 9.3$ T($\parallel b$) by the saturation recovery method. The recovery of the longitudinal magnetization $M_z(t)$ towards the equilibrium magnetization M_∞ was fitted by the expression [29],

$$M_z(t) = M_\infty - (M_\infty - M(0)) \times \left\{ A\exp\left(-\frac{t}{T_1}\right) + (1-A)\exp\left(-\frac{\lambda t}{T_1}\right)\right\}. \qquad (3)$$

Parameters A and λ are equal to 0.1 and 6 respectively for the central transition of a spin $I = \frac{3}{2}$ with non-zero electric field gradients (EFG) when the relaxation is purely magnetic [29].

The transverse relaxation was measured by the spin-echo decay method and the spin echo amplitude as a function of the time τ between the first $\pi/2$ and the second π pulse was fitted above 150 K by the following expression,

$$E(2\tau) = E(0)\exp\left[-2\tau/T_{2\rm L} - 0.5(2\tau/T_{2\rm G})^2\right] \qquad (4)$$

where $T_{2\rm G}$ is the Gaussian time associated with the nuclear spin-spin coupling through the conducting electrons and $T_{2\rm L}$ is the Lorentzian spin-echo time which reads, $1/T_{2\rm L} = 3(1/T_1)_b + (1/T_1)_{a,c}$.

3 Results

3.1 Knight shifts

Figures 1–3 show the T dependences of the ^{63}Cu NMR shift $^{63}K_b$ in samples $Sr_{14-x}Ca_xCu_{24}O_{41}$ and $La_5Ca_9Cu_{24}O_{41}$ under ambient and also at high pressures after subtraction of the small quadrupolar contribution in equation (2).

The NMR shift consists of two contributions; the orbital $K_{\rm orb}$ and spin $K_{\rm s}$ (Knight shift) contributions,

$$K_b(T) = K_{b,\rm orb} + K_{b,\rm s}(T) \qquad (5)$$

which can both be pressure and temperature dependent although no temperature dependence is expected for the orbital contribution. The second term $K_{b,\rm s}(T)$ is proportional to the uniform spin susceptibility $\chi_{\rm s}(T)$,

$$K_{b,\rm s}(T) = A_b(q=0)\chi_{\rm s}(T). \qquad (6)$$

The hyperfine form factor for the Cu_2O_3 ladders, $A_b(q)$, can be written as,

$$A_b(q) = A_b + 2B_b\cos q_x a + B_b\cos q_y a \qquad (7)$$

$$A_b(q=0) = A_b + 3B_b \qquad (8)$$

where A_b and B_b are the on-site and supertransferred hyperfine fields, respectively. For a separate estimate of $K_{b,\rm orb}$ and $K_{b,\rm s}$ we assume $K_{b,\rm s} = 0$ at $T = 0$ due to the presence of a spin gap in the spectrum of spin excitations. Then, $K_{b,\rm orb} = K_b(T=0)$.

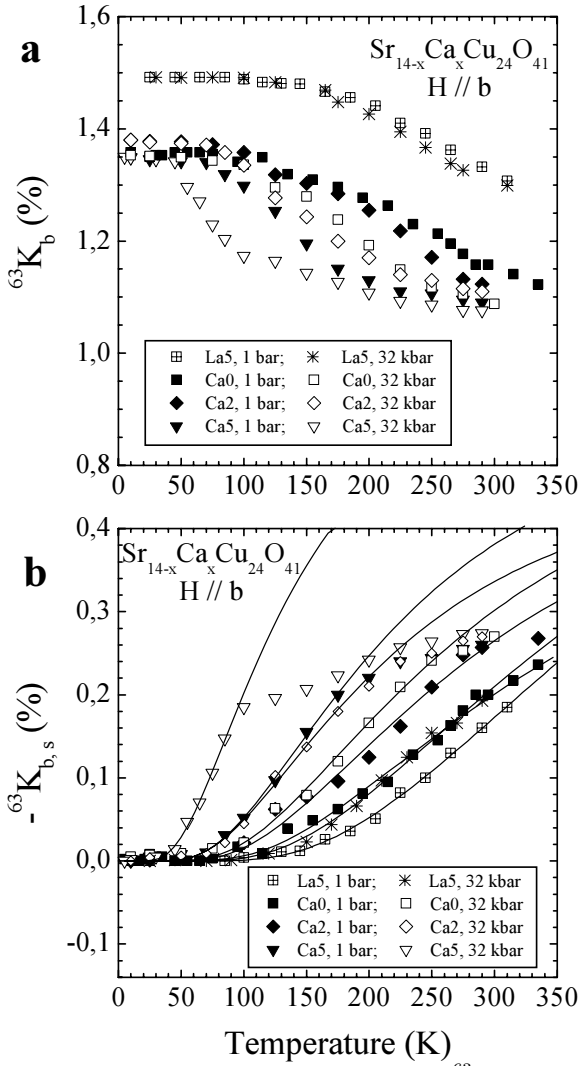

Fig. 1. (a) Temperature dependences of the ^{63}Cu NMR shift $^{63}K_b$ in $La_5Ca_9Cu_{24}O_{41}$ (La5) and $Sr_{14-x}Ca_xCu_{24}O_{41}$ ($x = 0, 2, 5$) for $H \parallel \mathbf{b}$ under ambient and high pressures. (b) T dependences of the ^{63}Cu Knight shift $^{63}K_{b,s}$ in $La_5Ca_9Cu_{24}O_{41}$ (La5) and $Sr_{14-x}Ca_xCu_{24}O_{41}$ ($x = 0, 2, 5$) for $H \parallel \mathbf{b}$ under ambient and high pressures. The lines are the fits to the data using equation (10).

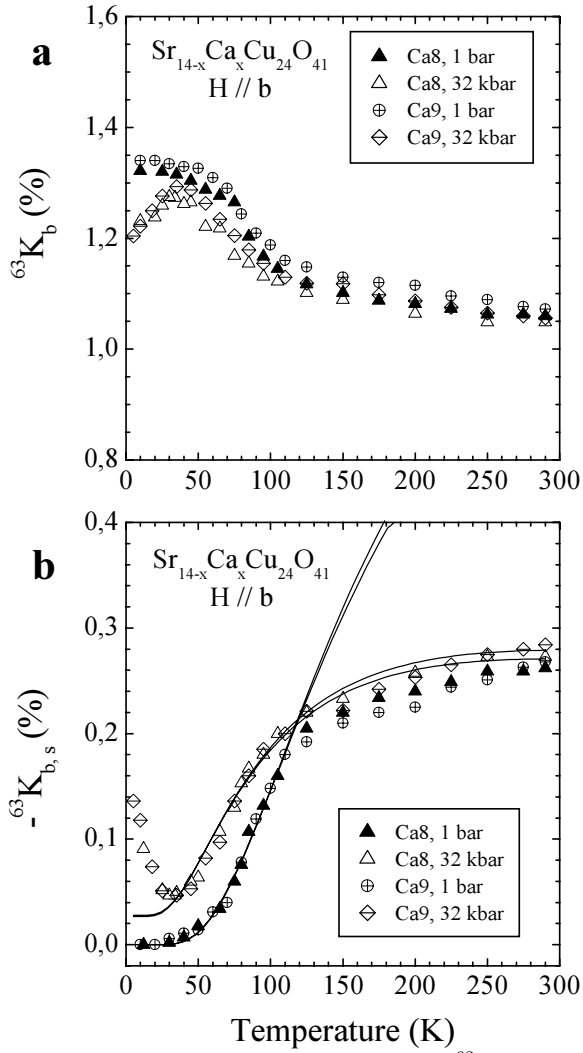

Fig. 2. (a) Temperature dependences of the ^{63}Cu NMR shift $^{63}K_b$ in $Sr_{14-x}Ca_xCu_{24}O_{41}$ ($x = 8, 9$) for $H \parallel \mathbf{b}$ under ambient and high pressures. (b) T dependences of the ^{63}Cu Knight shift $^{63}K_{b,s}$ in $Sr_{14-x}Ca_xCu_{24}O_{41}$ ($x = 8, 9$) for $H \parallel \mathbf{b}$ under ambient and high pressures. The lines are the fits to the data using equation (10).

A previous NMR study of $Sr_2Ca_{12}Cu_{24}O_{41}$ under pressure [30,20] has argued that the pressure induced increase of the Knight shift at low temperature with the concomitant suppression of the spin gap announced in our preliminary works [19,24] could actually be ascribed to the orbital part of the shift decreasing under pressure. It was proposed that the reduction of the orbital shift could be due to a reduction of the number of holes in the Cu-3$d_{x_2-y_2}$ orbital being transferred from Cu to O sites under pressure.

All our data of NMR shifts show a similar line position (between 1.32% and 1.39%) at low temperature under ambient pressure irrespective of the amount of Ca substitution for the entire $Sr_{14-x}Ca_xCu_{24}O_{41}$ series, (see Figs. 1a, 2a), [9]. Unlike the data presented in reference [20] the pressure dependence of the NMR shift is much larger at low temperature than at room temperature (0.18%) resp. (0.05%) at 36 kbar, see Figure 3a and therefore cannot be ascribed to a temperature independent pressure dependence of the orbital shift. In addition, according to the data presented in reference [20] we should have obtained a reduction of 0.18% for $K_{b,\mathrm{orb}}$ at $P = 36$ kbar. Our results of Figure 3a would thus impose the spin part $K_{b,\mathrm{s}}$ to be reduced by a factor about two at room temperature and 36 kbar, an assumption which we find unlikely. We can thus claim that all pressure dependences of NMR shifts for the $Sr_{14-x}Ca_xCu_{24}O_{41}$ series are attributable to the spin part.

Interestingly, we have found that $K_{b,\mathrm{orb}}$ in $La_5Ca_9Cu_{24}O_{41}$, Figure 1a, ($K_{b,\mathrm{orb}} = 1.49\%$) is appreciably larger than $K_{b,\mathrm{orb}}$ in the $Sr_{14-x}Ca_xCu_{24}O_{41}$ series which may be associated with a difference in symmetry and magnitude of crystalline fields in this compound.

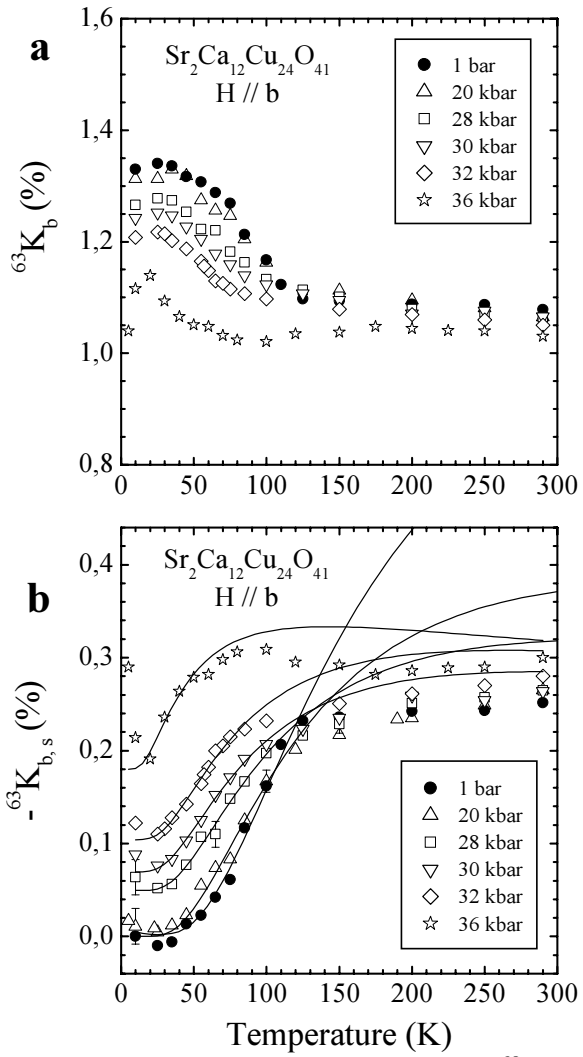

Fig. 3. (a) Temperature dependences of the ^{63}Cu NMR shift $^{63}K_b$ in $Sr_2Ca_{12}Cu_{24}O_{41}$ for $H \parallel \mathbf{b}$ at different pressures. (b) T dependences of the ^{63}Cu Knight shift $^{63}K_{b,s}$ in $Sr_2Ca_{12}Cu_{24}O_{41}$ for $H \parallel \mathbf{b}$ at different pressures. The lines are the fits to the data using equation (10).

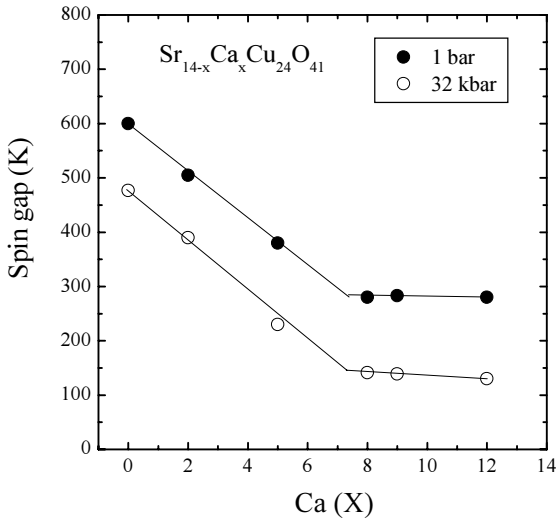

Fig. 4. Dependence of the spin gap Δ_s upon Ca substitution under ambient and high pressure. The values of Δ_s were obtained from the fits to the Knight shift data using equation (10). The solid lines are a guide for the eye.

The interesting feature in Figure 1a is the finding of rather similar values at high temperature and also at low temperature independent of x and of the applied pressure whereas big changes are observed in the intermediate temperature regime. For more heavily Ca-substituted samples Ca8, 9 and 12, Figures 2a, 3a, the story is quite different since the low temperature part becomes strongly affected by a change of x and also by the pressure. We notice an only small pressure dependence of $K_b(T)$ at $T > 150$ K which is *at variance* with the strong dependence observed at lower temperature. Consequently, we can again assume the pressure dependence of $K_{b,\mathrm{orb}}$ to be negligible and the spin contribution to the NMR shift can be derived by the following equation,

$$K_{b,\mathrm{s}}(P,T) = K_b(P,T) - K_{b,\mathrm{orb}}. \qquad (9)$$

The data of $K_{b,\mathrm{s}}$ are shown in Figures 1b, 2b and 3b. For lightly doped samples, the pressure (up to 32 kbar) does not affect the Knight shift at low temperature (which remains zero). This is *at variance* with what is occurring when the Ca content overcomes $x = 8$. Then, the spin part of the shift becomes pressure dependent at low temperature and a significant upturn of the NMR shift is observed at very low temperature although essentially under high pressure. No such effects are observed in lightly Ca-doped samples. The pressure dependence of the zero temperature shift in Ca12, Figure 3b, is indicative for the appearance of low-lying spin excitations above 20 kbar. This situation is reminiscent of the growth of zero frequency spectral weight which is observed in the undoped two-leg ladders upon substitution of Cu^{2+} by non-magnetic impurities [28,31]. A marked Curie-tail associated with the center of the spectrum is observed at low temperature under pressure in all samples with $x > 5$. Since this Curie contribution is not detected at ambient pressure in the same samples we feel confident that it cannot be attributed to impurities or instrumental shifts of the magnetic field. There is also an intermediate regime in which $K_{b,\mathrm{s}}(T)$ is activated. The scope of the present paper will be limited to the temperature regime in which Knight shifts are activated. An other paper will be devoted to low lying spin excitations and the occurrence of low temperature line shifts and broadenings.

We shall assume that the temperature dependence of $K_{b,\mathrm{s}}$ can be ascribed to the spin excitations above the spin gap Δ_s as for the undoped two-leg ladders. Hence, we fit the spin part $K_{b,\mathrm{s}}(T)$ using the following Troyer expression, valid in the low temperature domain [32],

$$K_{b,\mathrm{s}}(T) = \frac{C}{\sqrt{T}} \exp \frac{-\Delta_s}{T} \cdot \qquad (10)$$

The values of Δ_s thus obtained *via* fitting the data to equation (10) for Ca0, Ca2, Ca5, Ca8 and Ca12 at ambient and under a pressure of 32 kbar are displayed in Figure 4. The effect of pressure is large at all Ca contents. The relative reduction of Δ_s under pressure is steadily increasing with the density of holes (*vide infra*).We note that the data at ambient pressure agree fairly well with those published in

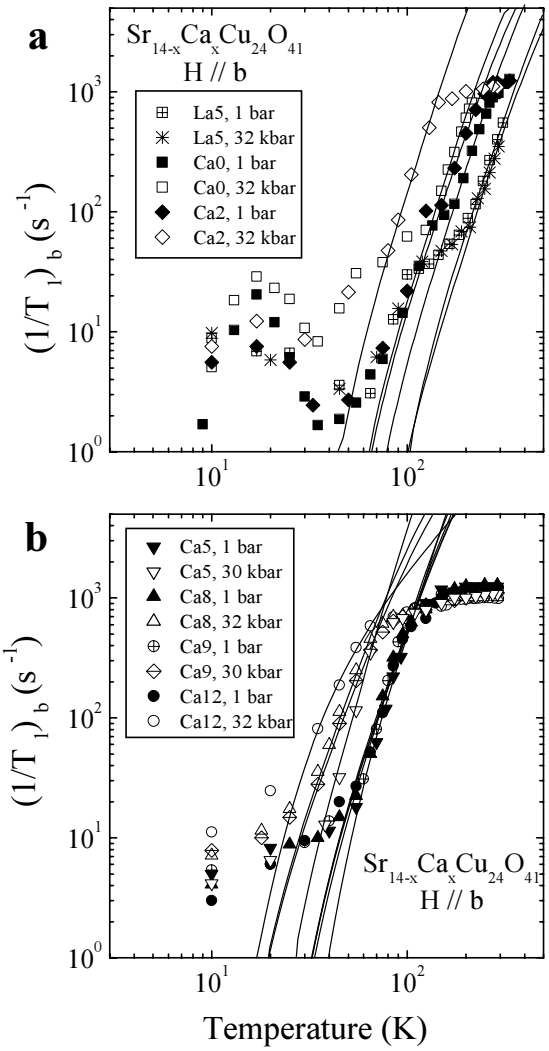

Fig. 5. (a) Temperature dependences of the spin lattice relaxation rate $^{63}T_1^{-1}$ in $La_5Ca_9Cu_{24}O_{41}$ (La5) and $Sr_{14-x}Ca_xCu_{24}O_{41}$ ($x = 0, 2$) for $H \parallel \mathbf{b}$ under ambient and high pressures. The lines are the fits to the data using equation (6). (b) Temperature dependences of the spin lattice relaxation rate $^{63}T_1^{-1}$ in $Sr_{14-x}Ca_xCu_{24}O_{41}$ ($x = 5, 8, 9$) for $H \parallel \mathbf{b}$ under ambient and high pressures. The lines are the fits to the data using equation (14).

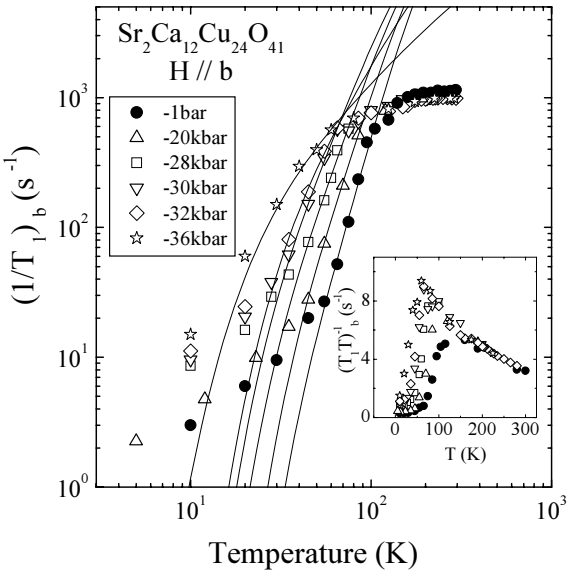

Fig. 6. Temperature dependences of the spin lattice relaxation rate $^{63}T_1^{-1}$in $Sr_2Ca_{12}Cu_{24}O_{41}$ for $H \parallel \mathbf{b}$ at different pressures. The lines are the fits to the data using equation (14). In the inset, $(T_1T)^{-1}$ *vs.* T.

reference [15]. The spin gap value of 840 K which is obtained for La5 is significantly larger than the results of undoped Cu_2O_3 ladders which are obtained through the ^{17}O Knight shift in $La_6Ca_8Cu_{24}O_{41}$, ($\Delta_s = 510$ K) [33] or by susceptibility in the $SrCu_2O_3$ structure [7]. However, these results fit rather well with our overall doping dependence of the spin gap in hole-doped ladders pertaining to the $(Sr/Ca)_{14}Cu_{24}O_{41}$ series which is presented in the present work.

3.2 Spin lattice and Gaussian relaxation

Temperature dependences of the spin-lattice relaxation rate $^{63}T_1^{-1}$ for $B(9.3\text{ T}) \parallel b$ axis at various pressures are displayed in Figures 5a, b and 6. It should be noted that the recovery curve of the nuclear magnetization was best fitted above ∼70 K according to equation (3) with a single T_1 component and with values for the A coefficients very close to values expected for magnetic relaxation of the central line in the presence of strong quadrupolar coupling, namely $A = 0.1$.

$$M_z(t) = M_\infty - (M_\infty - M(0)) \times \left\{ A \exp\left(-\frac{t}{T_1}\right) + (1-A)\exp\left(-\frac{6t}{T_1}\right)\right\} \cdot \quad (11)$$

A look at Figures 5a, b and 6 reveals at glance the clear existence of several different regimes for the temperature dependence of the relaxation rate in agreement with previous studies of hole-doped spin ladders, [15,19,34]. In all samples there is an activated regime in ranges depending on the Ca content which breaks down at low T. Below 30 K we can clearly see the emergence under pressure of a contribution to $1/T_1$ which is linear in temperature (Korringa-like) when x exceeds the value 8. This low temperature domain has been considered earlier in reference [19] and will be the subject of a further reinvestigation. Moreover, $1/T_1$'s for all $Sr_{14-x}Ca_xCu_{24}O_{41}$ compounds become nearly T-independent at high temperature and show a tendency to increase under pressure.

Figures 7a, b display the T dependence of the Gaussian component of the spin-echo decay rate $1/T_{2G}$ measured with $B \parallel b$ at different pressures. We observe that $1/T_{2G}$ increases gradually on cooling and is suppressed by increasing pressure and doping. The determination of $1/T_{2G}$ is no longer possible below 150 K in the heavily doped samples, ($x \geq 5$). This is due to a drastic shortening of T_2 at low temperature which prevents the derivation of the Gaussian component.

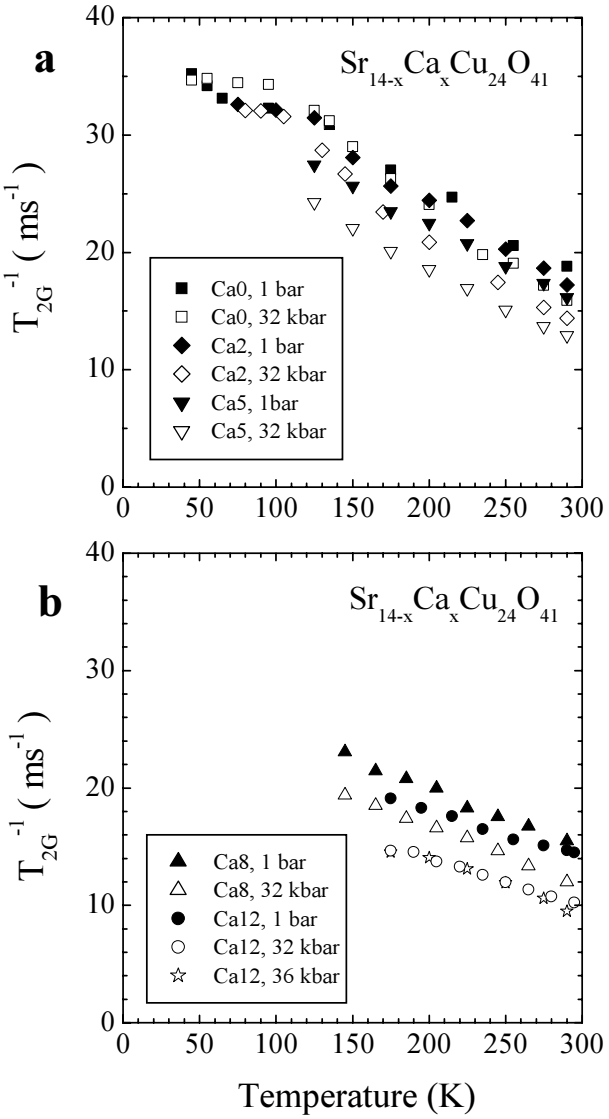

Fig. 7. (a) T dependences of the Gaussian component of the spin-echo decay rate T_{2G}^{-1} in lightly doped $Sr_{14-x}Ca_xCu_{24}O_{41}$ ($x = 0, 2, 5$) for $H \parallel \mathbf{b}$ under ambient and high pressure. (b) T dependences of the Gaussian component of the spin-echo decay rate T_{2G}^{-1} in heavily doped $Sr_{14-x}Ca_xCu_{24}O_{41}$ ($x = 8, 12$) for $H \parallel \mathbf{b}$ under ambient and high pressure.

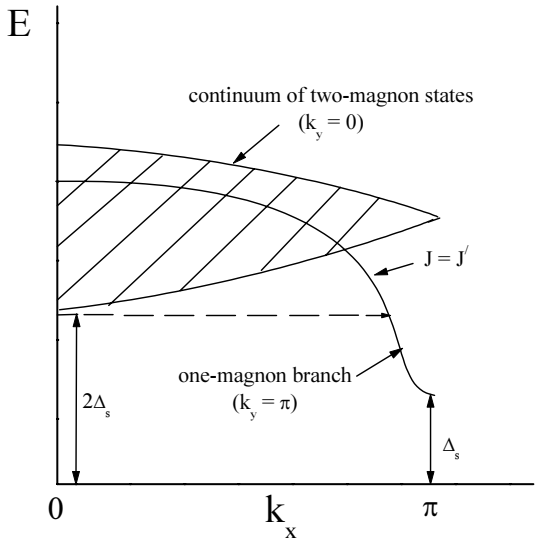

Fig. 8. Qualitative picture of the dispersion for $J_\perp \gg J_\parallel$ (dashed line) and for $J_\parallel = J_\perp$ (solid line). Hatched region corresponds to the continuum of two-magnon states at $k_y = 0$ and with minimum energy $2\Delta_s$. Three-magnon processes with momentum transfer $q_x \approx \pi$, $q_y = \pi$ consist in the scattering of an excited state belonging to the two-magnon continuum at the energy $2\Delta_s$ near $k_x = 0, k_y = 0$ into a state located on the single magnon dispersion branch (dashed line on the figure).

4 Interpretation

4.1 The isolated spin ladder model

4.1.1 Knight shifts

The purpose of this section is to examine how the observed Knight shifts can be related to the spin excitations of the $(Sr/Ca)_{14}Cu_{24}O_{41}$ spin ladders since $K_{b,s}(T)$ is likely to be governed by these excitations. There are first the spin excitations present in the undoped limit, *i.e.* excitations localized on the rung triplets in the strong coupling limit which give rise to a degenerate one-magnon band starting at the energy Δ_s for $k \cong (\pi, \pi)$ when the coupling along the legs is switched on. There is also a two-magnon continuum starting at the energy J, (see Fig. 8). These magnon excitations are indeed very robust against the weakening of the rung coupling since at intermediate coupling $J_\perp/J_\parallel \approx 0.5$ the spin gap is still of order $0.2J_\parallel$ [35]. Furthermore the magnon gap is also robust against doping up to 0.25 hole per Cu site *albeit* a significant decrease is observed as expected from the theory [17]. There is also an other kind of triplet spin excitations which must be considered when spin ladders are doped. They consist of hole pairs on the same rung dissociating into two individual quasiparticles on different rungs [36]. The role of quasiparticles on the NMR data will be discussed elsewhere.

In the gapped regime we shall assume that low lying excited states correspond to the excitations of single magnon modes with $k_x \approx \pi$, $k_y = \pi$ at the energy Δ_s. These modes govern the temperature dependence of the susceptibility, leading to the Troyer formula [32]. We may notice as pointed out in reference [32] that the formalism leading to equation (10) applies only to the very low temperature regime. In particular, the repulsion between magnons which prevent two magnons from occupying the same rung is not properly taken into account and is essential to get a correct temperature dependence.This may be a reason explaining why Troyer's formula is followed only up to about $\Delta_s/2$ in Figures 1b and 2b.

Values for the spin gap derived from a fit of the experimental data in Figures 1b, 2b, 3b with the Troyer formula are displayed in Figure 4 *versus* Ca content at $P = 1$ bar and $P = 32$ kbar. Figures 5a, b, 6 tell us that the spin gap is steadily decreasing upon Ca doping as long as x is smaller than 8. As established by the optical spectral

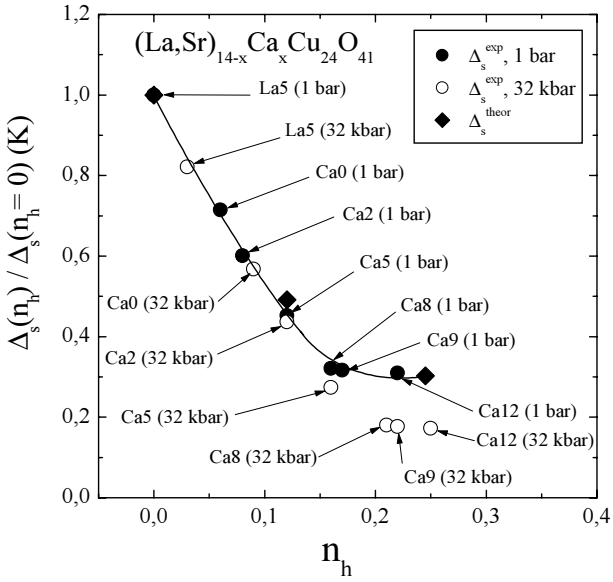

Fig. 9. The spin gaps $\Delta_{\rm s}^{\rm exp}$ and $\Delta_{\rm s}^{\rm theor}$ normalized to the undoped ladder value $\Delta_{\rm s}(n_h = 0)$ La5 (see text for details) as a function of the hole density n_h. The values of $\Delta_{\rm s}^{\rm exp}$ were obtained for various doping level from Knight shift measurements under ambient and high pressure. $\Delta_{\rm s}^{\rm theor}$ is the gap calculated for a two-chain Hubbard model using the density matrix renormalization group by Noack *et al.* [17]. The solid line is a guide for the eye.

weight data, Ca doping amounts to a redistribution of the holes between chains and ladders [9].

The main effect of Ca doping on the structure is a reduction of the b parameter. A similar conclusion is reached by analyzing the effect of hydrostatic pressure. This is the b parameter which is most sensitive to pressure. Hence, using the spin gap *versus* x displayed in Figure 4 and structural data under pressure [37], we are in a position to establish a correspondence between the respective roles of pressure and calcium doping. The contraction of the lattice parameters induced by a pressure of $P = 30$ kbar corresponds to the additional substitution of three Sr by three Ca, *i.e.* $b(x, P = 30\ \text{kbar}) \approx b(x+3, P = 1\ \text{bar})$ [37]. We can attribute the decrease of $\Delta_{\rm s}$ upon Ca substitution in Figure 4 to a transfer of holes from the chains to the ladders. We can also use the doping calibration curve to plot the variation of $\Delta_{\rm s}$ against the hole density in the ladders. This plot is displayed in Figure 9 where spin gaps at each Ca doping levels have been normalized by the experimental value of the gap in the La5 compound at ambient pressure, 840 K. Furthermore, we have assumed a negligible amount of holes in the ladders of the La5 sample under ambient pressure, given the average Cu valence of 2.04 and the distribution of holes between chains and ladders in Ca0 which supports the dominant role of holes in the chains. Subsequently all gaps have been normalized to the undoped ladder value.

The amplitude of the intraladder coupling although unknown in La5 should not depart strongly from the values obtained in layered cuprates or the undoped $SrCu_2O_3$ ladder, namely $J_{\parallel} \approx 1600$ K leading in turn to $\Delta_{\rm s}/J_{\parallel} = 0.5$. The numerical results for the Heisenberg ladder [35] would thus correspond to $J_{\perp}/J_{\parallel} \approx 1$ which is a reasonable value in the undoped ladder limit. This is consistent with the anisotropy ratio which has been derived from the interpretation of the neutron scattering data in La6 introducing a smaller four-spin exchange interaction [38]. As pressure is increased we can expect some redistribution of the holes to take place between chains and ladders with a maximum concentration for the holes on the ladders reachable under pressure corresponding to the uniform situation, namely 0.04. Using the measured value of the spin gap in La5 and taking $n_{\rm h}$ (1 bar) = 0, the plot of Figure 9 suggests that the density of holes in the La5 ladders amounts to $n_{\rm h} = 0.03$ under 32 kbar. We have also assumed in Figure 9 the ladder hole density reaching the saturation value of 0.25 in Ca12 under pressure.

The data in Figure 9 have been compared to the calculation of the gap for a two-chain Hubbard model using the density matrix renormalization group [17]. We notice a good agreement between the theory and the experimental data at ambient pressure. However, the agreement is no longer satisfying at 32 kbar when x is larger than 8. We are thus forced to look for an other source of pressure dependence for the spin gap in Ca-rich (strongly hole-doped) samples.

We notice a persistent discrepancy between the determinations of the spin gap by NMR and inelastic neutron spectroscopy (INS). Several attempts to measure the spin gap in pristine and Ca-substituted samples of the $Sr_{14-x}Ca_xCu_{24}O_{41}$ series by inelastic neutron spectroscopy have provided a gap of about 32–35 meV in all compounds independent of the Ca concentration [10,39,40,21]. The disagreement is even more striking in La5, 6 when spin gaps are measured by the two techniques [38]. Since neutron data have been obtained at low temperature it could be argued that finite temperature effects could affect the determination of the spin gap *via* susceptibility and relaxation time measurements *via* magnon damping possibly enhanced by the dissociation of quasiparticle pairs [41]. However the comparison between neutron and susceptibility data remains a major challenge in the physics of doped spin ladders. Furthermore, no pressure dependence could be detected by neutron spectroscopy in Ca rich samples [22]. What is badly needed now is a neutron measurement of the spin excitations in the pressure domain $30 - 40$ kbar.

What is most remarkable in Figure 3b is the existence of a finite value for the Knight shift at low temperature in Ca12 at pressures larger than 20 kbar. This contribution is also visible in samples with a smaller Ca content although only in the high pressure limit. A small contribution is still observed in Ca8 under 32 kbar but the zero temperature Knight shift of Ca5 would not depart from zero even under pressure, see Figure 1b. A finite zero temperature Knight shift is the signature of low-lying spin excitations. A look at Figure 3b and 4 suggests that the onset of a zero temperature Knight shift corresponds to a critical value of the spin gap ≈230 K. The low temperature Knight shift

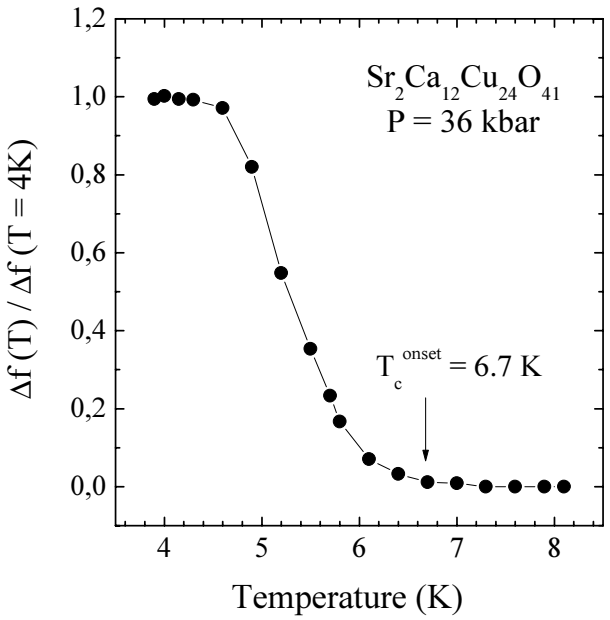

Fig. 10. T dependence of the tuning frequency shift $\Delta f(T)$ of the NMR resonant circuit caused by a superconducting transition in $Sr_2Ca_{12}Cu_{24}O_{41}$ at 36 kbar. $\Delta f(T)$ has been normalized to the maximum value of the shift $\Delta f_{\max} = \Delta f(T = 4\ \mathrm{K})$.

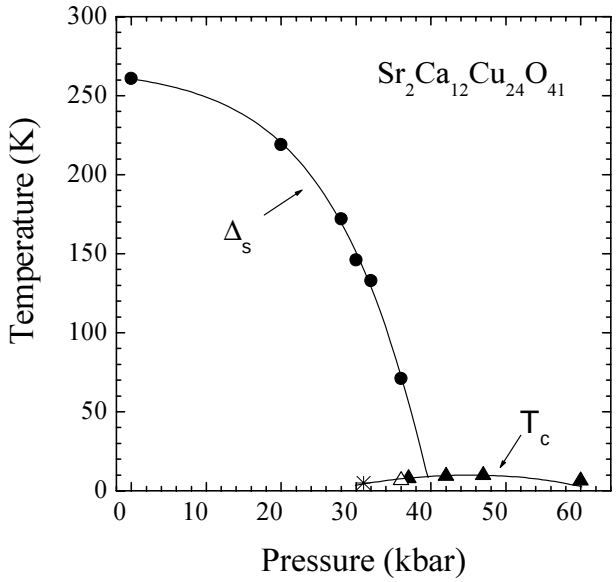

Fig. 11. Pressure dependence of the spin gap Δ_s obtained from the fits to the Knight shift data using equation (10) and of the superconducting transition temperature, T_c, for $Sr_{2.5}Ca_{11.5}Cu_{24}O_{41}$ (△) [2] and for $Sr_2Ca_{12}Cu_{24}O_{41}$ (∗) [19], (▲) [62].

has been the subject of an extensive pressure study only in Ca12 samples. The data show a steady increase of the low temperature Knight shift above 20 kbar going along with a decrease of the spin gap displayed in Figure 4.

We have used the same NMR resonant circuit to look for superconductivity in Ca12 under 36 kbar without any magnetic field applied. The onset of the tuning frequency shift occurs at 6.7 K, see Figure 10. In spite of a small signal due to an NMR circuit which is not optimized for the detection of superconductivity we take it as the signature of the superconducting ground state under 36 kbar. The onset temperature given by AC methods is known to be one or two degrees below the transition temperature obtained by the onset of the resistive transition when the transition is not extremely narrow. Hence this AC result at 36 kbar is in fair agreement with the accepted phase diagram for superconductivity [42]. Most interesting in Figure 11 displaying the pressure dependence of Δ_s and T_c is the coexistence under 36 kbar of superconductivity at 6.7 K with a finite spin gap of 80 K and a large zero temperature Knight shift.

4.1.2 Spin-lattice relaxation time

Our first attempt to understand the spin lattice relaxation data presented in Figures 5a, b and 6 will be to examine how far one can go into the interpretation using magnon modes of the undoped spin ladder corresponding to spin triplet excitations.

The single-magnon modes which govern the temperature dependence of the susceptibility are located at an energy equal at least to the gap Δ_s and consequently the energy conservation law cannot be fulfilled in the scattering process since the nuclear Larmor frequency ω_0 is much smaller than Δ_s. The only relevant relaxation channels are those which are quasi-elastic and involve a scattering between two excited magnon states. The channel with both magnons in the region $k_x \approx \pi$, $k_y = \pi$ with momentum transfer $q \sim (0,0)$, see Figure 8, leads to the relaxation,

$$\frac{1}{T_1} \sim \mid A_{q=0} \mid^2 \ \mathrm{e}^{-\frac{\triangle_{T_1}}{T}} \qquad (12)$$

at low temperature ($T \ll \Delta_s$) [32], with the assumption of a quadratic dispersion law for the excitations of undoped Heisenberg ladders in the case of $J_\perp \geq J_\parallel$.

It is well known that there exists a discrepancy between derivations of gaps $\Delta_{T_1}$and Δ_s. A similar activation energy for T_1 and Knight shift is measured in the undoped organic Heisenberg ladder $Cu_2(C_5H_{12}N_2)_2Cl_4$ [43] in agreement with the theoretical predictions [32,44]. However, in all doped ladder systems Δ_{T_1} extracted from T_1 is about 1.5 times larger than the gap Δ_s obtained from $K_{b,s}$, [7,14,15,19,45,46]. The possible reasons for the difference between Δ_{T_1} and Δ_s are under intense discussion. We intend to propose an interpretation which allows understanding relaxation data on the basis of a spin gap from Knight shift experiments only.

As emphasized by Troyer *et al.* [32] a contribution to $^{63}T_1^{-1}$ at low T should come from the two-magnon process with momentum transfer $q \sim (0,0)$ which requires the minimum energy Δ_s. However, Sandvik and Dagotto [47] have pointed out the possibility for three-magnon processes with momentum transfer $q_x \approx \pi$, $q_y = \pi$ to be equally efficient in the relaxation. These processes consist in the scattering of an excited state belonging to

the two-magnon continuum at the energy $2\Delta_s$ near $k_x = 0, k_y = 0$ into a state located on the single magnon dispersion branch with momentum transfer $q_x \approx \pi,\ q_y = \pi$, (see Fig. 8). This contribution can be large because the ladder has strong short-range AF correlations [22,48,49]. The numerical studies carried out by Sandvik *et al.* [47] have concluded to contributions $(\frac{1}{T_1})_{q=0}$ and $(\frac{1}{T_1})_{q=\pi}$ being of comparable magnitudes at temperatures such as $T \sim \triangle_s$. Furthermore it was shown in references [47,50] that the main contribution to $1/T_1$ in the temperature range $T > \Delta_s$ comes from three-magnon processes with momentum transfers $q_x \approx \pi,\ q_y = \pi$.

Recently Ivanov and Lee [50] have suggested that $^{63}T_1^{-1}$ is determined in the experimentally relevant temperature range by the sum of $(\frac{1}{T_1})_{q=0}$ and $(\frac{1}{T_1})_{q=\pi}$ contributions with comparable weights. In the low temperature limit, $(T < \Delta_s)$, they have found the expression for the contribution to $1/T_1$ coming from the processes with $q \cong (\pi, \pi)$ namely,

$$(\frac{1}{T_1})_{q=\pi} \sim \frac{T}{\triangle_s}\, \mathrm{e}^{-\frac{2\triangle_s}{T}}. \tag{13}$$

Consequently, we have fitted our $1/T_1$ data by the form,

$$\frac{1}{T_1} = \left(\frac{1}{T_1}\right)_{q=0} + (\frac{1}{T_1})_{q=\pi} \propto C_0 \exp\left(-\frac{\triangle_s}{T}\right) + C_\pi \left(\frac{T}{\Delta_s}\right) \exp\left(-\frac{2\triangle_s}{T}\right). \tag{14}$$

Equation (14) represents the analytic form of the low T asymptotics of the two and three-magnons processes which should apply in the temperature domain $T/\Delta_s < 0.5$ in which such an approximation is justified. The solid lines in Figures 5a, b are a fit according to equation (14) using the gap value $\triangle_s$ derived from the Knight shift data and a ratio $\frac{C_\pi}{C_0} = 70$. The agreement is fairly good in the gapped regime and equation (13) leads to $(\frac{1}{T_1})_{q=\pi} = 4.76(\frac{1}{T_1})_{q=0}$ at $T/\Delta_s = 0.5$. The ratio of the two contributions to the relaxation is practically independent of the Ca concentration as long as low lying excitations are absent. However this interpretation breaks down when a finite contribution to the Knight shift arises at low temperature (*i.e.* in Ca-rich samples under pressure) with the concomitant occurrence of a new source of relaxation.

A calculation of the relaxation has been performed by Naef and Wang [51] using the transfer density matrix renormalization group method for AF couplings relevant in spin ladders. These authors were able to separate the $q = (0,0)$ and $q = (\pi, \pi)$ contributions and concluded to the necessary contribution of the $q = (\pi, \pi)$ channel for understanding the cross-over observed in $^{63}T_1^{-1}$ data of undoped ladders. Using the experimental data $(\frac{1}{T_1})_{q=\pi} = 4.76(\frac{1}{T_1})_{q=0}$ at $T/\Delta_s = 0.5$ together with an interpolation of the Naef and Wang calculation, the ratio $\frac{J_\perp}{J_\parallel}$ would correspond to 0.9. This anisotropy is fairly consistent with our data of spin gap in $La_5Ca_9Cu_{24}O_{41}$ (the half-filled band situation), $\Delta_s = 840$ K, using the relation between the spin gap and the anisotropy calculated by the Heisenberg spin ladder model [35]. This anisotropy ratio is not however in agreement with the interpretation of the INS experiments leading to an anisotropy of 0.72 [21] in Ca11.5 and 0.55 in Ca0 [40]. A similar discrepancy between neutron and NMR techniques has been noticed in the discussion of the Knight shift data. We may suggest that the spin gap is severely suppressed by hole doping going from La5 to Ca12 samples while the exchange couplings are much less affected.

According to the theory, [51] the cross-over between gapped and paramagnetic regimes of isolated chains should be located around $T/\Delta_s = 0.6$. With amplitudes for the gaps obtained from the Knight shift data, the cross-over regime thus derived is in fair agreement with the temperature dependences of $1/T_1$ displayed in Figures 7a, b, 8 since the relaxation rate becomes nearly temperature independent at high temperature as expected above the cross-over temperature.

It can be noted that our results agree well with those of the ^{17}O and ^{63}Cu NMR experiments for undoped $La_6Ca_8Cu_{24}O_{41}$ and $Sr_{14-x}Ca_xCu_{24}O_{41}(x = 0, 12)$ obtained by Fujiyama *et al.* [41]. As is well known, magnon processes for the momentum transfer $q \cong (\pi, \pi)$ do not contribute to $^{17}T_1^{-1}$ because of the filtering of low frequency spin fluctuations at $q \cong (\pi, \pi)$ by the hyperfine form factor $^{17}G(q)$ for oxygen sites in the ladders (see Ref. [33,41]). Using the different q-dependences of the hyperfine form factors for O and Cu sites Fujiyama *et al.* [41] have shown that the relaxation process at the Cu sites is dominated by spin excitations near $q = (\pi, \pi)$ even when the temperature is lower than the spin gap. Moreover, they have revealed that singlet correlations along the rungs in the heavily doped compound Ca12 become drastically weaker above a certain temperature and that such a behavior is most likely caused by the dissociation of bound hole pairs.

4.2 Transverse coupling

We have seen in Section 4.1.1 that the hole doping being a function of the Ca content and also of the pressure can explain the x dependence of Δ_s for all x values at ambient pressure and its pressure dependence provided x remains smaller than 8. Consequently for the large x regime, $(x > 8)$, we must look for an other mechanism which is likely to suppress Δ_s when the pressure is increased. Recently, Imada and Iino [52] have studied the effect of the interladder coupling, J_L, on the critical magnetic properties of spin ladder systems using the scaling theory together with quantum Monte Carlo calculations. They have shown that the spin gap is very sensitive to the ratio $J_L/J_\parallel$. As discussed above, a large variation of the intrachain coupling constant, $J_\parallel$, under pressure seems to be unlikely. We can use the model of Imada and Iino [52] for the case of coupled undoped ladders with an isotropic exchange and no non magnetic impurities. With the value of $J_\parallel$ derived from inelastic neutron data

in $Sr_{2.5}Ca_{11.5}Cu_{24}O_{41}$, $J_\parallel = 990 \pm 160$ K [21] (the argument would not be ruined by using $J_\parallel = 1500$ K) and the dependence $\Delta_s/J_\parallel$ *versus* $J_L/J_\parallel$ obtained in reference [52] we estimate that the reduction of Δ_s from 260 K at 1 bar to 70 K at 36 kbar in Ca12 corresponds to the increase of J_L from 220 K ($J_L/J_\parallel = 0.20$) to 330 K ($J_L/J_\parallel = 0.30$).

We can notice the agreement between these estimates and the predictions made in references [53,54] for the ratio $J_L/J_\parallel \sim 0.1 \div 0.2$ using a perturbation theory. Consequently, the pressure dependence of Δ_s in the Figure 11 could possibly be explained by the increase of J_L. Thus, it is likely that the spin gap suppression under pressure in the $Sr_{14-x}Ca_xCu_{24}O_{41}$ series results from a combination of hole density and interladder coupling increase.

5 The Gaussian relaxation

The $1/T_{2G}$ Gaussian rate in copper oxides is related to the magnetic correlation length ξ of the spin fluctuations, [55,56]. Furthermore, the actual relationship between ξ and T_{2G} is determined by the dimensionality of the materials. It has been found that $T_{2G} \propto \xi^{-\frac{1}{2}}$ for $1D$ spin chains [57,58] and $T_{2G} \propto (T\xi)^{-1}$ for $2D$ systems [33]. As to the relation between T_{2G} and ξ dependence in quasi-$1D$ two-leg ladders, Magishi *et al.* [15] have suggested for the case of an isotropic intra-ladder coupling, $J_\parallel = J_\perp$, the following form,

$$T_{2G}^2 = \alpha + \beta\xi_{\text{ladder}}^{-1}. \tag{15}$$

The T dependence of ξ_{ladder}^{-1} in two-leg ladders has been studied by Greven *et al.* [58] who have obtained the relation,

$$\xi_{\text{ladder}}^{-1} = \frac{2}{\pi}\Delta_s + AT\exp\left(-\frac{\Delta_s}{T}\right), \tag{16}$$

in the limit $J_\perp \leq J_\parallel$ where Δ_s is a spin gap from the Knight shift data. Using equations (15) and (16) the T dependence of T_{2G}^2 can be expressed as,

$$T_{2G}^2 = A_0 + BT\exp\left(-\frac{\Delta_s}{T}\right) \tag{17}$$

where $A_0 = T_{2G}^2(T=0) \sim \xi_0^{-1} \sim \Delta_s$ *i.e.* the saturation value of the correlation length due to the finite spin gap.

$T_{2G}^2(T)$ data as a function of Ca content and pressure are displayed in Figures 12a, b. Solid lines are the fits to the data using equation (16) and the values of Δ_s derived from Knight shift measurements. The overall agreement of our data with those of reference [15] at ambient pressure is rather satisfactory. We can also notice a rise of $T_{2G}^2(T=0)$ with increasing Ca content although this growth is not linear with respect to the Ca doping.

Magishi *et al.* [15] have suggested that the spin correlation length ξ in hole-doped ladders can be affected by the existence of holes in the ladders. Hence, $T_{2G}^2(T=0) \sim \xi_{\text{eff}}^{-1} = \xi_h^{-1} + \xi_o^{-1}$ where ξ_h is a correlation length related to the average distance between holes whereas ξ_o is the intrinsic correlation length of the ladder related to the spin gap. ξ_o^{-1} is likely to depend on pressure since it is proportional to the spin gap and ξ_h^{-1} must depend on the hole concentration *i.e.* on both Ca content and pressure since we have found in this work an equivalence between Ca doping and pressure. The data of Figure 12a suggest that for lightly Ca-doped samples ($x \leq 5$) ξ_h^{-1} and ξ_o^{-1} are of similar order of magnitude with opposite pressure dependences leading in turn to an accidental insensitivity of $T_{2G}^2(T=0)$ to pressure. However, heavily doped samples are in the dirty limit, $\xi_h^{-1} \gg \xi_o^{-1}$, and the increase of

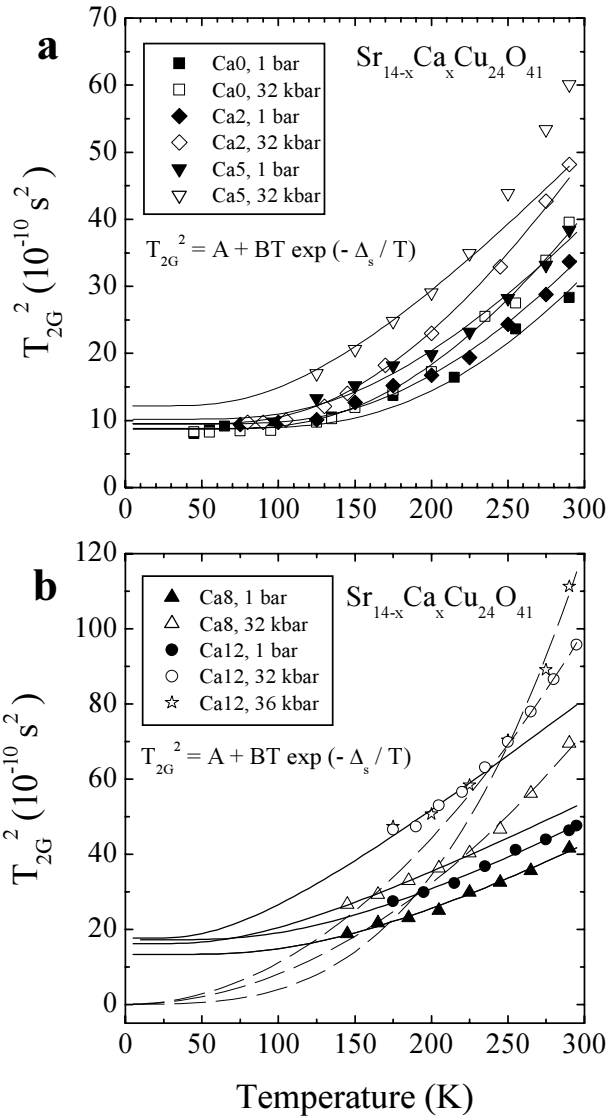

Fig. 12. (a) T_{2G}^2 as a function of T in $Sr_{14-x}Ca_xCu_{24}O_{41}$ ($x = 0, 2, 5$) for $H \parallel \mathbf{b}$ at $P = 1$ bar and $P = 32$ kbar. The lines are the fits to the data using equation (17) with Δ_s derived from Knight shift measurements. (b) T_{2G}^2 as a function of T in $Sr_{14-x}Ca_xCu_{24}O_{41}$ ($x = 8, 12$) for $H \parallel \mathbf{b}$ under ambient and high pressures. The solid lines are the fits to the data using equation (17). The dashed lines are the fits to the data using equation (19).

$T^2_{2G}(T=0)$ under pressure corresponds to an increase in the density of holes, see for instance the data for $x=8$ in Figure 12b. Consequently, a change of Δ_s by pressure no longer affects $T^2_{2G}(T=0)$ in doped compounds.

However, the T dependence of T^2_{2G} in heavily doped compounds becomes strongly affected by pressure, see *e.g.* data of Ca8 and 12 in Figure 12b. We see that the whole T dependence of T^2_{2G} for ladders with $x \geq 5$ at high P cannot be fitted by a single expression such as equation (17). The fit of the high T part of the data (above say $T=250$ K) by equation (17) leads to the unphysical negative values of $T^2_{2G}(T=0)$ while the fit of data in the T range below $T=250$ K gives reasonable quantities for $T^2_{2G}(T=0)$. The increase of $T^2_{2G}(T=0)$ in Ca5 and Ca8 under pressure is thus mainly governed by the increase of n_h in the ladder planes of those compounds. $T^2_{2G}(T=0)$ becomes nearly insensitive to pressure in Ca12 as a result of n_h reaching saturation in Ca12 under pressure.

Quite recently, Thurber *et al.* [59] have shown that the behavior of T^2_{2G} for isolated two- and three-leg ladders at elevated temperatures is given by,

$$T^2_{2G} \propto T^2 \xi^{-1}. \tag{18}$$

Consequently, by combining equations (17) and (18) we obtain the following form for the description of the high T behavior of T^2_{2G},

$$T^2_{2G} = AT^2 + BT^3 \exp\left(-\frac{\Delta_s}{T}\right). \tag{19}$$

As is seen in Figure 12b, T^2_{2G} data above 250 K (at high pressure) can be rather well fitted by the equation (19) (dashed lines). Thus, the T_{2G} data for $x=5,8$ and 12 compounds under pressure are described by assuming the existence of a dimensional cross-over at T_{cross} for the functional dependence of T^2_{2G} with respect to ξ^{-1}. The temperature domain below the cross-over temperature corresponds to a regime of 2-leg ladders where the spin gap is influenced (decreased) by the inter-ladder interaction. This is relevant only for Ca8 and 12 samples under pressure.

The kink which is observed between solid and dashed lines for Ca8 and 12 samples in Figure 12b can be attributed to the manifestation of a cross-over involving the interladder coupling between the low and high temperature regimes in the ξ dependence of T^2_{2G}.

It can be noticed that the values of T_{cross} relative to Δ_s strongly depends on x [60]. This dependence is understood in the following manner. T^2_{2G} behaves as $T^2_{2G} \propto T^2\xi^{-1}$ only above the temperature where the ladders can be considered as isolated entities, *i.e.* at $T \sim J_L$, (the inter-ladder coupling). Therefore, T_{cross} becomes a function of both Δ_s and J_L. We can expect an increase of J_L at increasing pressure following the discussion in Section 4.2 and also with Ca content leading in turn to an increase of T_{cross}/Δ_s. The cross-over temperature is such as $T_{cross} \geq \max(J_L, \Delta_s)$. The temperature dependence of T^2_{2G} in Ca12 under pressure, Figure 12b, suggests a cross-over temperature above 250 K which would be in fair agreement with the estimate $J_L \approx 150-300$ K derived in Section 4.2 from the value of the spin gap taking into account the inter-ladder coupling interaction.

6 Spin gap and superconductivity

A feature of the $P-T$ phase diagram (Fig. 11) that deserves a special consideration is the existence of a maximum of the superconducting critical temperature when pressure drives the characteristic energy scales for pair binding energy and the spin gap down to values of the order of T_c. Beyond this optimal pressure for the highest T_c, denoted as P_{opt}, these intra-ladder gaps become irrelevant and hence T_c decreases under pressure. The latter pressure domain is also characterized by a temperature dependence of resistivity along the inter-ladder a direction that becomes metallic [61,62]. Such a change of behavior in T_c can be seen as a cross-over from strong to weak coupling conditions for long-range superconducting order.

Arguments in support of this viewpoint follow from simple considerations about mechanisms of long-range superconducting order in coupled ladder systems. Let us consider in the first place the region below P_{opt} where the gaps are larger than T_c; in this domain, long-range superconducting coherence perpendicular to ladder leg direction can only be achieved through a Josephson coupling. An analysis based on the renormalized perturbation theory [63] shows that the Josephson coupling takes the form of

$$J_s \approx 2\frac{\xi_s}{c}\frac{t_L^2}{T^*}, \tag{20}$$

where $\xi_s \approx t_\parallel/T^*$ stands as the size of the superconducting hole pairs within the ladders, while t_L is the inter-ladder single electron hopping ($t_L \ll t_\parallel$). This expression contains the usual term t_L^2/T^* for the effective transverse motion of the pairs requiring an intermediate energy of order T^* (the confinement temperature of hole pairs on ladders, see Sect. 1) and a factor ξ_s/c that accounts for the increase in probability for pair hopping due to delocalization of holes forming the pairs along the ladder direction [63]. As for pair correlations of isolated ladders, they are well known to be strongly enhanced in the presence of a spin gap. Numerical and analytical results for $t-J$ and repulsive Hubbard models for example [64,65], show that "d-wave" pair susceptibility follows a power law $\chi_s(T) \sim (T/\Delta_s)^{-\gamma_s}$ for temperatures below the spin gap, where $\gamma_s \approx 1$. A molecular-field approximation of the Josephson coupling that rigorously takes the influence of intra-ladder correlations into account, allows one to obtain at once an expression for the transition temperature. Thus from the condition $J_s\chi_s(T_c)=1$ one finds,

$$T_c \sim t_L^2/T^*, \tag{21}$$

which assumes that $\Delta_s \sim T^*$. It follows that T_c increases when T^* decreases, a feature that is essentially governed by the increase of the Josephson coupling under pressure.

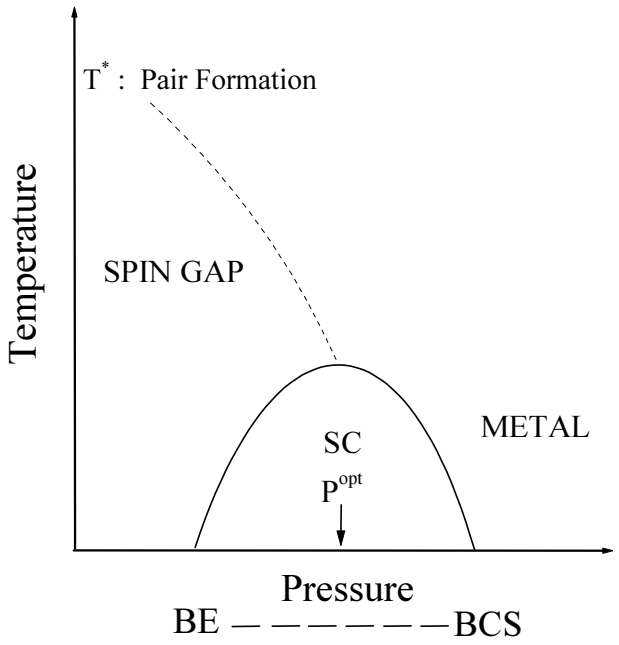

Fig. 13. Qualitative phase diagram of the pair formation temperature T^* and superconducting transition temperature T_c as a function of the pressure.

Now when pressure is further increased, one reaches the domain where $T_c \sim T^*$ and a change in the physical picture of the transition occurs. The gaps are no longer relevant for the mechanism promoting long-range order and its description evolves toward a weak coupling picture − a situation that bears close similarities with the antiferromagnetic ordering of quasi-one-dimensional organic conductors with a charge gap under pressure[4]. When the metallic character of the normal state is well developed along longitudinal and transverse directions the motion of the holes is likely to be coherent along both directions leading to Fermi liquid conditions − or deconfinement of holes, in agreement with the restoration of a metallic transverse resistivity. Thus sufficiently above P_{opt}, the transition temperature should follow from a weak coupling BCS prescription which yields

$$T_c \approx t_L e^{-1/|g*|}. \quad (22)$$

Here g^* is the residual attractive coupling between deconfined holes. Since pressure weakens the strength of short-range superconducting correlations, it will lead to a decrease of $|g^*|$ at the energy scale t_L for deconfinement [66,63]. This in turn reduces T_c as a function of pressure. It follows then that a maximum of T_c is expected when the ladder system evolves from strong to weak coupling conditions for hole pairing at $P \sim P_{opt}$. A qualitative description of the pressure profile of T_c and Δ_s is summarized in Figure 13.

7 Conclusion

The present work has reported a ^{63}Cu-NMR study of the spin gap structure and of the spin excitations under pressure of the doped Cu_2O_3 ladders in the $(Sr/Ca)_{14}Cu_{24}O_{41}$ family covering a wide range of hole doping. A similar study has been performed with the compound $La_5Ca_9Cu_{24}O_{41}$ in which the ladders are nearly undoped. The spin gap at ambient pressure is found to decrease steadily from La5 ($\Delta_s = 840$ K) to Ca8 ($\Delta_s = 300$ K) as x is increased and more smoothly at larger Ca concentration up to Ca12. Comparing the effect of pressure on the spin gap and on the lattice parameters enables us to explain the x and P dependences of the spin gap in the low Ca doping range by the evolution of the hole doping from 0.028 up to 0.15 from Ca0 to Ca8. A pressure of 32 kbar does not alter the spin excitations qualitatively when $x < 8$ since the susceptibility is still reaching a zero value at low temperature. However in Ca rich samples, pressure promotes the existence of low lying spin excitations giving rise to a finite susceptibility at low temperature.

The salient result of this study is the coexistence in the Ca12 sample under the pressure of 36 kbar of gapped spin excitations (with a gap of 80 K) with superconductivity at 6.7 K. The results of the present work provide a further confirmation to the early study published by Mayaffre *et al.* [19] although the actual title of reference [19] may appear as somewhat misleading in the light of coexisting gapped and low lying spin excitations.

These new results are supporting the exciting prospect of superconductivity induced by the interladder tunneling of preformed pairs [53,67,66] at least in the pressure domain where the pressure remains smaller than the pressure corresponding to the maximum of the critical temperature for superconductivity.

After the study of the spin-lattice relaxation of ^{63}Cu nuclei in the $Sr_{14-x}Ca_xCu_{24}O_{41}$ series for various levels of Ca substitution and also under pressure we are able to identify two different temperature regimes. A fairly consistent interpretation of the spin lattice relaxation data above 50 K is obtained by taking into consideration two and three-magnon modes relaxation channels responsible for the activated nuclear relaxation in the gapped temperature regime and a quasi-1D spin dynamics at high temperature. Using a linear combination between two and three magnon modes enables us to remove the discrepancy between activation energies obtained from susceptibility and $1/T_1$ experiments.

The dependence of the Gaussian relaxation time has confirmed that the rise of the correlation length at low temperature is limited by two factors; the quantum limitation due to the finite spin gap and the average distance between holes. It is the second factor which prevails in Ca-rich samples under pressure. A kink in the temperature dependence of $1/T_{2G}$ at high pressure in heavily doped samples has been attributed to the manifestation of a cross-over between the behavior of isolated ladders at high temperature and the behavior of coupled ladders at low temperature.

Doped cuprate spin ladders in which the doping can be controlled by pressure are remarkable prototype compounds for the study of the mechanism for superconductivity in cuprates. The interplay between the real space pair binding and superconductivity can also be studied. Experiments at even higher pressures where a more conventional kind of superconductivity is expected would be most useful.

Y.P acknowledges the French Ministry of Research and CNRS for a postdoctoral financial support. We thank J.P. Boucher for a useful discussion. A BQR grant from the Université Paris-Sud is also acknowledged.

References

1. M. Uehara *et al.*, J. Phys. Soc. Jpn **656**, 2764 (1996).
2. T. Nagata *et al.*, Physica C **282-287**, 153 (1997).
3. E. Dagotto, T.M. Rice, Science **271**, 618 (1996).
4. C. Bourbonnais, D. Jérome, in *Adv in Synthetic Metals* (Elsevier, 1999), p. 206.
5. E.M. Mc Carron *et al.*, Mater. Res. Bull. **23**, 1355 (1988).
6. T. Siegrist, L.F. Schneemeyer, S.A. Sunshino, J.V. Wasczak, R.S. Roth, Mater. Res. Bull. **23**, 1429 (1988).
7. M. Azuma, Z. Hiroi, M. Takano, K. Iohida, Y. Kitaoka, Phys. Rev. Lett. **73**, 3463 (1994).
8. R.S. Roth *et al.*, J. Am. Chem. Soc. **72**, 1545 (1989).
9. T. Osafune *et al.*, Phys. Rev. Lett. **78**, 1980 (1997).
10. L.P. Regnault *et al.*, Phys. Rev. B **59**, 1055 (1999).
11. N. Motoyama *et al.*, Phys. Rev. B **55**, 3386 (1997).
12. T. Nagata *et al.*, Phys. Rev. Lett. **81**, 1090 (1998).
13. E. Dagotto, J. Riera, D. Scalapino, Phys. Rev. B **45**, 5744 (1992).
14. K. Kumagai, S. Tsuji, M. Kato, Y. Koike, Phys. Rev. Lett. **78**, 1992 (1997).
15. K. Magishi *et al.*, Phys. Rev. B **57**, 11533 (1998).
16. M. Takigawa, N. Motoyama, H. Eisaki, S. Uchida, Phys. Rev. B **57**, 1124 (1998).
17. R.M. Noack, S.R. White, D.J. Scalapino, Phys. Rev. Lett. **73**, 882 (1994).
18. D. Poilblanc, H. Tsunetsugu, T.M. Rice, Phys. Rev. B **50**, 6511 (1994).
19. H. Mayaffre *et al.*, Science **279**, 345 (1998).
20. T. Mito *et al.*, Physica B **259-261**, 1042 (1999).
21. S. Katano *et al.*, Phys. Rev. Lett. **82**, 636 (1999).
22. S. Katano *et al.*, Physica B **259-261**, 1046 (1999).
23. The compound $La_6Ca_8Cu_{24}O_{41}$ would have been an even better choice to provide the reference undoped ladder system but the sample quality was not as good as for the $La_5Ca_9Cu_{24}O_{41}$ single crystals.
24. Y. Piskunov *et al.*, Eur. Phys. J. B **13**, 417 (2000).
25. G.B. Benedek, T. Kushida, J. Phys. Chem. Solids **5**, 241 (1958).
26. J.F. Baugner, P.C. Taylor, T. Oja, P.J. Bray, J. Chem. Phys. **50**, 4914 (1969).
27. R.B. Creel *et al.*, J. Chem. Phys. **60**, 2310 (1974).
28. N. Fujiwara *et al.*, Phys. Rev. Lett. **80**, 604 (1998).
29. A. Narath, Phys. Rev. **162**, 320 (1967).
30. Y. Kitaoka *et al.*, in *Physics and Chemistry of Transistion-Metal Oxides*, Springer series in Solid State Sciences (Springer-Verlag, 1999), p. 299.
31. G.B. Martins, E. Dagotto, J. Riera, Phys. Rev. B **54**, 16032 (1996).
32. M. Troyer, H. Tsunetsugu, D. Wurtz, Phys. Rev. B **50**, 13515 (1994).
33. T. Imai, K.R. Thurber, K.M. Shen, A.W. Hunt, F.C. Chou, Phys. Rev. Lett. **81**, 220 (1998).
34. Y. Kitaoka *et al.*, J. Magn. Magn. Mater. **177-181**, 487 (1998).
35. T. Barnes *et al.*, Phys. Rev. B **47**, 3196 (1993).
36. H. Tsunetsugu *et al.*, Phys. Rev. B **49**, 16078 (1994).
37. S. Pachot *et al.*, Phys. Rev. B **59**, 12048 (1999).
38. M. Matsuda *et al.*, Phys. Rev. B **62**, 8903 (2000).
39. R.S. Eccleston, M. Azuma, M. Takano, Phys. Rev. B **53**, 14721 (1996).
40. R.S. Eccleston *et al.*, Phys. Rev. Lett. **81**, 1702 (1998).
41. S. Fujiyama, M. Takigawa, N. Motoyama, H. Eisaki, S. Uchida, J. Phys. Soc. Jpn **69**, 1610 (2000).
42. T. Nakanishi *et al.*, J. Phys. Soc. Jpn **67**, 2408 (1998).
43. G. Chaboussant *et al.*, Phys. Rev. Lett. **70**, 925 (1997).
44. J. Sagi, I. Affleck, Phys. Rev. B. **53**, 9188 (1996).
45. K. Ishida, Y. Kitaoka, K. Asayama, M. Azuma, Z. Hiroi, M. Takano, J. Phys. Soc. Jpn **63**, 322 (1994).
46. S. Tsuji *et al.*, J. Phys. Soc. Jpn **65**, 3474 (1996).
47. A.W. Sandvik, E. Dagotto, D. Scalapino, Phys. Rev. B **53**, R2934 (1996).
48. S. Ohsugi *et al.*, Phys. Rev. Lett. **82**, 4715 (1999).
49. T. Nagata *et al.*, J. Phys. Soc. Jpn **68**, 2206 (1999).
50. D.A. Ivanov, P.A. Lee, Phys Rev. B **59**, 4803 (1999).
51. F. Naef, X. Wang, Phys. Rev. Lett. **84**, 1320 (2000).
52. M. Imada, Y. Iino, J. Phys. Soc. Jpn **66**, 568 (1997).
53. T.M. Rice, S. Gopolan, M. Sigrist, Europhys. Lett. **23**, 445 (1993).
54. S. Gopolan, T.M. Rice, M. Sigrist, Phys. Rev. B **49**, 8901 (1994).
55. C.H. Pennington *et al.*, Phys. Rev. B **39**, 274 (1989).
56. C.H. Pennington, C.P. Slichter, Phys. Rev. Lett. **66**, 381 (1991).
57. S. Sachdev, Phys. Rev. B **50**, 13006 (1994).
58. M. Greven, R.J. Birgeneau, U.J. Wiese, Phys. Rev. Lett. **77**, 1865 (1996).
59. K.R. Thurber *et al.*, Phys. Rev. Lett. **84**, 558 (2000).
60. $T^{\rm cross}(x = 5, P = 32$ kbar$) \approx \Delta_{\rm s}$; $T^{\rm cross}(x = 8, P = 32$ kbar$) \approx 1.5\Delta_{\rm s}$; $T^{\rm cross}(x = 12, P = 32$ kbar$) \approx 2\Delta_{\rm s}$; $T^{\rm cross}(x = 12, P = 36$ kbar$) \approx 3\Delta_{\rm s}$.
61. N. Mori *et al.*, Physica B **239**, 137 (1997).
62. P. Auban-Senzier *et al.*, Synthetic Metals **103**, 2632 (1999).
63. C. Bourbonnais, L.G. Caron, Int. J. Mod. Phys. B **5**, 1033 (1991).
64. C.A. Hayward, D. Poilblanc, R.M. Noack, D.J. Scalapino, W. Hanke, Phys. Rev. Lett. **75**, 926 (1995).
65. H.J. Schulz, Phys. Rev. B **53**, 2959 (1996).
66. J. Kishine, K. Yonemitsu, J. Phys. Soc. Jpn **67**, 1714 (1998).
67. J. Kishine, K. Yonemitsu, J. Phys. Soc. Jpn **66**, 3725 (1997).